The International Journal of Biochemistry & Cell Biology 45 (2013) 141–150

Contents lists available at SciVerse ScienceDirect

The International Journal of Biochemistry & Cell Biology

journal homepage: www.elsevier.com/locate/biocel

Disrupted ATP synthase activity and mitochondrial hyperpolarisation-dependent oxidative stress is associated with p66Shc phosphorylation in fibroblasts of NARP patients☆

Magdalena Lebiedzinska[a,1], Agnieszka Karkucinska-Wieckowska[b,1], Aleksandra Wojtala[a,1], Jan M. Suski[a,c], Gyorgy Szabadkai[d], Grzegorz Wilczynski[a], Jakub Wlodarczyk[a], Catia V. Diogo[a,e], Paulo J. Oliveira[e], Jan Tauber[f], Petr Ježek[f], Maciej Pronicki[b], Jerzy Duszynski[a], Paolo Pinton[c], Mariusz R. Wieckowski[a,*]

[a] Nencki Institute of Experimental Biology, Warsaw, Poland
[b] Department of Pathology, The Children's Memorial Health Institute, Warsaw, Poland
[c] Department of Experimental and Diagnostic Medicine, Section of General Pathology, Interdisciplinary Centre for the Study of Inflammation (ICSI) and LTTA Centre, University of Ferrara, Ferrara, Italy
[d] Department of Cell and Developmental Biology, University College London, Consortium for Mitochondrial Research, London, United Kingdom
[e] CNC – Centre for Neuroscience and Cell Biology, University of Coimbra, Coimbra, Portugal
[f] Dept. No. 75, Institute of Physiology, Academy of Sciences of the Czech Republic, Prague, Czech Republic

ARTICLE INFO

Article history:
Available online 31 July 2012

Keywords:
p66Shc
NARP
Mitochondria
Reactive oxygen species
Antioxidant defence

ABSTRACT

p66Shc is an adaptor protein involved in cell proliferation and differentiation that undergoes phosphorylation at Ser36 in response to oxidative stimuli, consequently inducing a burst of reactive oxygen species (ROS), mitochondrial disruption and apoptosis. Its role during several pathologies suggests that p66Shc mitochondrial signalling can perpetuate a primary mitochondrial defect, thus contributing to the pathophysiology of that condition. Here, we show that in the fibroblasts of neuropathy, ataxia and retinitis pigmentosa (NARP) patients, the p66Shc phosphorylation pathway is significantly induced in response to intracellular oxidative stress related to disrupted ATP synthase activity and mitochondrial membrane hyperpolarisation. We postulate that the increased phosphorylation of p66Shc at Ser36 is partially responsible for further increasing ROS production, resulting in oxidative damage of proteins. Oxidative stress and p66Shc phosphorylation at Ser36 may be mitigated by antioxidant administration or the use of a p66Shc phosphorylation inhibitor.

This article is part of a Directed Issue entitled: Bioenergetic dysfunction, adaptation and therapy.

1. Introduction

Many studies have suggested that p66Shc (an adaptor protein which belongs to the ubiquitous ShcA family) can be an important factor in ROS-related pathologies because of its participation in cellular pathways that respond to oxidative stress. Under physiological conditions, the involvement of ShcA proteins (p46Shc, p52Shc and p66Shc) in signal transduction pathways requires the phosphorylation of tyrosine residues located in their central CH1 domains by receptor tyrosine kinases (TRKs) (Pelicci et al., 1992; Lotti et al., 1996). The binding of tyrosine-phosphorylated p52 and p46 to the Grb/Sos complex facilitates Ras pathway activation. However, tyrosine-phosphorylated p66Shc counteracts the interaction of p52 and p46 with the Grb2/Sos complex and prevents Ras activation. In this case, p66Shc acts as a negative regulator of the proliferation pathway (Migliaccio et al., 1997; Khanday et al., 2006).

Apart its participation in signal transduction, p66Shc is involved in the regulation of mammalian lifespan and in the cellular response to the oxidative stress caused by reactive oxygen species (ROS), which is implicated in the pathogenesis of many diseases and the ageing process (Migliaccio et al., 1999). p66Shc possesses an additional CH2 domain that contains the Ser36 phosphorylation site (Luzi et al., 2000), which under oxidative stress conditions caused

☆ This article is part of a Directed Issue entitled: Bioenergetic dysfunction, adaptation and therapy.

* Corresponding author at: Laboratory of Bioenergetics and Biomembranes, Department of Biochemistry, Nencki Institute of Experimental Biology, Pasteur 3 St., 02-093 Warsaw, Poland. Tel.: +48 22 589 23 72.
E-mail address: m.wieckowski@nencki.gov.pl (M.R. Wieckowski).

[1] Equal contribution to this paper.

1357-2725/$ – see front matter © 2012 Elsevier Ltd. All rights reserved.
http://dx.doi.org/10.1016/j.biocel.2012.07.020

by various pro-oxidants and toxic agents is phosphorylated at Ser36 (Migliaccio et al., 1999; Pellegrini et al., 2005). The best-described pathway of p66Shc phosphorylation at Ser36 involves protein kinase C β2 (PKCβII) (Pinton et al., 2007), but this protein can also be phosphorylated by other kinases, including JNK (Le et al., 2001) and stress-activated protein kinases (SAPK) (Yang and Horwitz, 2002; Hu et al., 2005). The cellular response to oxidative stress involving p66Shc is a multi-step process (for details see Pinton et al., 2007) with the translocation of p66Shc to the mitochondria and/or mitochondria-associated membranes (MAM). This results in the intensification of ROS production by the mitochondria. The mechanism of p66Shc-related ROS production has not yet been fully determined. One hypothesis suggests that cytochrome c interacts with p66Shc in the mitochondrial intermembrane space (IMS) and is responsible for ROS generation (Giorgio et al., 2005). The presence of p66Shc in the MAM fraction, which physically interacts with the outer mitochondrial membrane (OMM), suggests that p66Shc can interact with some OMM proteins that have oxidoreductase activity (e.g., NADH-cytochrome b_5 reductase). This interaction may promote ROS production; however, such an assumption should be experimentally confirmed. Detailed studies of p66Shc biological activity have also revealed that this protein can influence antioxidant enzyme biosynthesis because p66Shc phosphorylation at Ser36 is associated with the inactivation of the FOXO3a factor (mammalian homolog of *C. elegans* lifespan determinant, DAF16). FOXO3a is a member of the group of forkhead transcription factors (FKHR-L) that binds to the promoters of the SOD2 and catalase genes in mammalian cells and activates their transcription. Under oxidative stress, FOXO3a is inactivated and restrained in the cytoplasm (Nemoto and Finkel, 2002; Purdom and Chen, 2003; Lam et al., 2006).

It has been demonstrated that p66Shc phosphorylation at Ser36 may be induced not only by external factors but also by endogenous oxidative stress related to mitochondrial dysfunction. In human fibroblasts with various molecular defects in mitochondrial protein synthesis, membrane phospholipids or respiratory chain subunits, deficiencies in bioenergetic parameters and antioxidant defence are associated with an apparent increase in the phosphorylation of p66Shc at the serine 36 residue. Interestingly, the inhibition of p66Shc phosphorylation by a PKCβ inhibitor partially decreases the oxidative stress in these cells (Lebiedzinska et al., 2010).

Neurodegenerative and age-associated diseases, cancer and diabetes involve an altered mitochondrial phenotype, which is associated with increased oxidative stress (Lebiedzinska et al., 2010; Pagnin et al., 2005; Zeviani and Di Donato, 2004). Mitochondrial disorders are hereditary, incurable pathologies that are caused by a variety of changes in mitochondrial or nuclear DNA that affect the mitochondrial metabolism and bioenergetics (Lenaz et al., 2004; Zeviani and Di Donato, 2004). It has also been proposed that mitochondrial pathologies, independently from their molecular background may lead to the dysfunction of the mitochondrial respiratory chain which can also cause ROS generation. One of the most recognized defects in this respect is the m.8993T>G mutation in subunit 6 of the mitochondrial ATP synthase (MTATP6) resulting in the substitution of a highly conserved leucine to arginine (L156R) (D'Aurelio et al., 2010). Despite of the heterogenic symptoms, this most common and studied mutation at mtDNA nucleotide 8993 is described by the acronym NARP based on the symptoms in the first described patient (neuropathy, ataxia, retinitis pigmentosa). In contrast to most other pathogenic (heteroplasmic) mtDNA mutations, the levels of m.8993T>G mutation do not vary significantly among different tissues in the same subject (Craig et al., 2007) which make fibroblast cultures of affected individuals an easy and reliable experimental tissue. Moreover, the NARP phenotype is observed when the mutation load varies between 70 and 90%. If higher, it may cause the fatal infantile encephalopathy (MILS). As it was proposed, enhanced production of ROS affects DNA, enzymes and phospholipids, which results in further abnormalities in mitochondrial function and exacerbates the pathology (Geromel et al., 2001). This feedback loop is customarily called the vicious cycle of ROS production (Mancuso et al., 2009). p66Shc has been found to be an important part of this pathologic vicious cycle.

In the present study, we tested the hypothesis that in fibroblasts from NARP patients, phosphorylation of p66Shc at Ser36 is a consequence of ROS overproduction due to hyperpolarisation of the inner mitochondrial membrane. We also postulate that p66Shc activation contributes to further mitochondrial oxidative stress. In fibroblasts from patients with NARP syndrome, the mitochondrial respiratory chain operates properly, but the protonmotive force is not used for ATP synthesis because of a defect in ATP synthase. The low ATP synthase activity is responsible for the mitochondrial hyperpolarisation and the resulting increased ROS production and p66Shc phosphorylation at Ser36. To prevent ROS-induced damage and to inhibit the p66Shc-related ROS vicious cycle, the effects of a PKCβ inhibitor (hispidin) and antioxidants, such as a vitamin E derivative (Trolox) and a plastochinon derivative (SkQ), were investigated. As there is currently no potential treatment for mitochondrial diseases, a decrease in oxidative stress in the cells harbouring the mitochondrial defect is desirable. The possible mechanisms and conditions of p66Shc Ser36 phosphorylation should be elucidated in detail to possibly prevent the harmful effects of p66Shc-related ROS generation in the presented model.

2. Results

2.1. Patients

To study the effect of p66Shc on the cellular response to mitochondria-related oxidative stress, fibroblast cultures were obtained from two patients with nearly homoplasmic 8993T>G (p.L156R) mtDNA mutations that caused a defect in subunit 6 of the ATP synthase (ATP6) and human neonatal dermal fibroblasts (Fn) used as a control. Patient 1 (P1) presented at the age of 3 months with truncal hypotonia and hypertonic jerks. Progressive neurological symptoms with a decrease in visual contact and increased plasma and cerebrospinal lactate levels were also observed. At the age of 5 months, the patient required artificial ventilation because of respiratory failure. Patient 2 (P2) showed epilepsy-like episodes at the age of 9 months and was treated with valproate. A deterioration of the neurological status in conjunction with lactic acidosis then developed. Brain MRI images at the ages of 9 and 18 months showed severe progressive atrophy. Muscle biopsies of the patients revealed non-specific histological and histochemical changes, although no OXPHOS abnormalities were found spectrophotometrically in the muscle homogenates. The mitochondrial pathology suspected in both patients was directly confirmed by the identification of a common mtDNA mutation of the MILS/NARP type in the DNA isolated from the muscle. Oil Red O staining of NARP fibroblasts revealed increased lipid deposits accumulation indicating an abnormal lipid metabolism (Supplementary Figure 1). However, the profile of the lipid metabolism enzymes (short chain hydroxyacyl CoA dehydrogenase, medium chain acyl CoA dehydrogenase and trifunctional protein) was not changed compared with the cells from human neonatal dermal fibroblasts (Fn) and human skin fibroblasts of healthy volunteer (C3). The muscle and fibroblast biopsies were performed at 6 and 25 months of age, respectively, in patients 1 and 2.

2.2. Bioenergetic characterisation and ROS production in fibroblasts from NARP patients

To determine the impact of the ATP synthase defect on the mitochondrial metabolism in fibroblasts from NARP patients, the mitochondrial membrane potential (mtΔΨ), respiratory chain activity and mitochondrial NADH redox index were measured. The measurement of mtΔΨ using the fluorescent probes TMRM and JC1 showed a slight increase in the proton-motive force in the mitochondria of the patients' fibroblasts (Fig. 1A and A′). The increased mtΔΨ correlated with a 20% decrease in electron transport chain activity (Fig. 1B) that was observed in these cells. The decrease in the respiratory chain activity related to the higher mtΔΨ was confirmed by the increased NADH redox index in the NARP fibroblasts (Fig. 1C). To extend the control group, we also studied the heterogeneity of the studied parameters in control fibroblasts. We used several other control groups, including two other cell lines: human adult dermal fibroblasts (C2) and human skin fibroblasts of healthy volunteer (C3) and compared several parameters with human neonatal dermal fibroblasts (Fn). The results presented in Supplementary Figure 2 show that human neonatal dermal fibroblasts used as the control do not differ significantly from the other control cell lines. The absolute NADH and FAD fluorescence levels are shown in Supplementary Figure 3. Increased mitochondrial superoxide anion (mt. $O_2^{\bullet -}$) production (Fig. 1D) correlated with the decrease of aconitase activity (Fig. 1G). Interestingly, we observed reduced cytosolic superoxide (cyt. $O_2^{\bullet -}$) and hydrogen peroxide (H_2O_2) production in both NARP fibroblast lines (Fig. 1E and F). The defect in ATP synthase was visualised using blue native gel electrophoresis and an in-gel activity assay. In both NARP cell lines, we observed decreased ATP synthase activity compared with control cells (Fig. 1I). Moreover, mitochondrial oxidative stress in the fibroblasts of NARP patients was responsible for the higher level of oxidatively damaged proteins, as indicated by the increased levels of protein carbonylation (Fig. 1H). In both NARP cell lines, we also detected decreased calcium uptake by the mitochondria ($6.73 \pm 1.27\ \mu M$, $2.8 \pm 0.54\ \mu M$ and $5.21 \pm 1.18\ \mu M$ for the control, P1 and P2 cells, respectively), which indicates that mitochondrial calcium homeostasis was affected. The standard cytochemical analysis of the fibroblasts of NARP patients is presented in Supplementary Figure 4.

2.3. Mitochondrial morphology in fibroblasts of NARP patients

Because most mitochondrial dysfunctions influence the structure of the mitochondrial network, we performed a detailed analysis of the static and dynamic mitochondrial network parameters using fluorescence microscopy and image analysis software. The mitochondrial morphology visualised by MitoTracker Red staining showed that the mitochondrial network in NARP cells was significantly fragmented (Fig. 2A). The image analysis (Fig. 2B) indicated that the mitochondrial area and volume in the fibroblasts of NARP patients were decreased compared with the control cells, whereas the subcellular distribution (dispersion) of the mitochondrial network in healthy and NARP cell lines was comparable.

2.4. p66Shc Ser36 phosphorylation status and the levels of antioxidant enzymes in fibroblasts of NARP patient

To investigate the possibility that mitochondrial alterations in fibroblasts from NARP patients, including increased oxidative stress are able to activate p66Shc phosphorylation at Ser36, we estimated the phosphorylation status of p66Shc. Western blotting revealed an increased level of p66Shc phosphorylated at Ser36 in the fibroblasts of NARP patients (Fig. 3A). The calculated ratio between Ser36-P-p66Shc and p66Shc indicated a significant increase in the phosphorylation of p66Shc (Fig. 3B). Moreover, in both patient cell lines, we observed an increased level of activated (e.g., phosphorylated at serine 660) PKCβ (Fig. 3C), which supports the p66Shc phosphorylation results. Based on the literature (Pani and Galeotti, 2011; Smith et al., 2005; Koch et al., 2008; Pani et al., 2009) and our previous results (Lebiedzinska et al., 2010) suggesting that Ser36-phosphorylated p66Shc influences antioxidant enzymes, we studied altered expression of antioxidant enzymes in the NARP model of intracellular oxidative stress. We determined that the level of SOD1 was unchanged, whereas the levels of SOD2 and GPx 1 and 2 were greatly increased. Surprisingly, an extremely low level of catalase was detected in both fibroblast lines with NARP mutations (Fig. 3A). FOXO3a, which is the main transcription factor responsible for the regulation of SOD2 and catalase expression, was found to be inactivated in NARP patient fibroblasts; this transcription factor is under the control of p66Shc (Fig. 3D). To mimic the ATP synthase dysfunction observed in fibroblasts from NARP patients, we induced mitochondrial hyperpolarisation by treating control fibroblasts with oligomycin. In this experimental model, the oligomycin-induced shift to mitochondrial state 4 respiration is coupled with mitochondrial hyperpolarisation and increased mitochondrial superoxide production (Suski et al., 2012). The treatment of control fibroblasts with oligomycin increased the phosphorylation of p66Shc at Ser36 (Supplementary Figure 5), which indicates a direct relationship among mitochondrial hyperpolarisation, oxidative stress and the phosphorylation of p66Shc at Ser36.

2.5. Effect of the inhibition of the p66Shc phosphorylation pathway on intracellular oxidative stress and mitochondrial parameters in NARP fibroblasts

To test the hypothesis that the phosphorylation of p66Shc at Ser36 is an important element in the oxidative stress-driven vicious cycle in cells harbouring NARP mutations, we inhibited p66Shc phosphorylation using the PKCβ-specific inhibitor hispidin. We observed that hispidin and two antioxidants (Trolox and SkQ) decreased the phosphorylation of p66Shc in NARP patient fibroblasts (Fig. 4 and Supplementary Figure 6). These observations correlated with the diminished mitochondrial superoxide production (Fig. 5A and B) observed after hispidin treatment of NARP fibroblasts. Comparing Trolox and SkQ differential effects were observed. Trolox decreased both mitochondrial and cytosolic superoxide anion in both NARP fibroblast lines. By its turn, SkQ had more limited effect, causing a significant mitochondrial superoxide anion decrease in P2 NARP fibroblast line.

3. Discussion

The production of oxygen free radicals by mitochondria has been implicated in several aspects of mitochondrial physiology, ranging from a physiological activation of signalling pathways to a deleterious initiation of mitochondrial degeneration and, ultimately, the induction of mitochondrial-mediated cell death (Jones, 2006; Kakkar and Singh, 2007; Kowaltowski et al., 2009; Pereira et al., 2009). p66Shc, which is an alternatively spliced isoform of the growth factor adaptor that belongs to the ShcA family, is a new player in the control of mitochondrial physiology and modulation of ROS production. This protein has received increasing attention in the last several years for its involvement in oxidative stress-induced mitochondrial alterations. p66Shc contains an additional domain, CH2, with a Ser36 phosphorylation site that is unique among Shc proteins. p66Shc phosphorylation at Ser36 triggers increased ROS production, which can contribute to mitochondrial damage under different stress conditions and aging (Lebiedzinska et al., 2009, 2010). Upon translocation to the mitochondria, p66Shc can

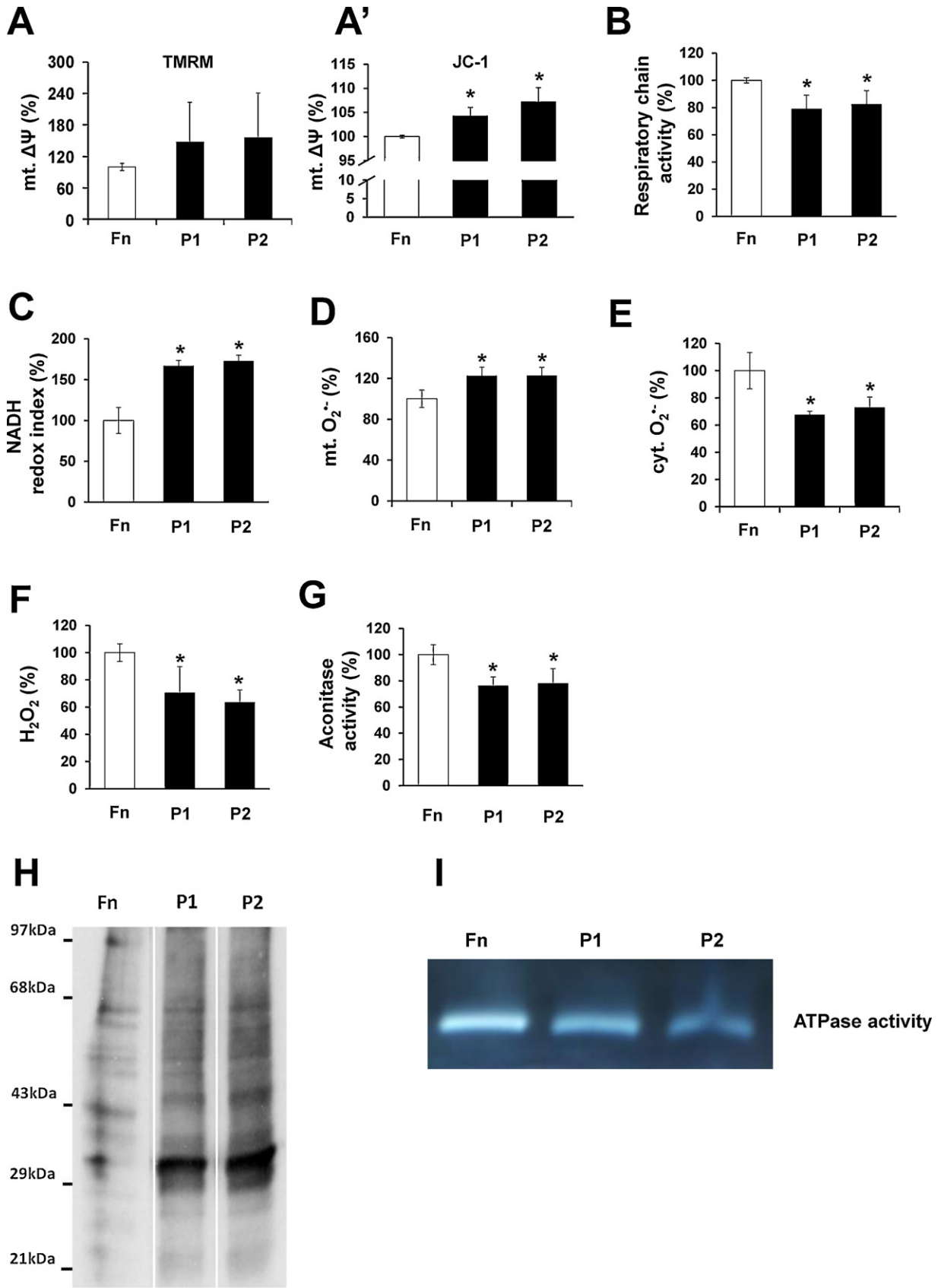

Fig. 1. Bioenergetic characterisation, ROS production and protein carbonylation in control and patient fibroblasts. (A) mitochondrial membrane potential (mtΔΨ) measured with the use of TMRM; (A′) mitochondrial membrane potential (mtΔΨ) measured with the use of JC-1; (B) respiratory chain activity; (C) redox index (NADH/NAD); (D) mitochondrial superoxide production ($mtO_2^{\bullet-}$); (E) cytosolic superoxide production ($cytO_2^{\bullet-}$); (F) hydrogen peroxide (H_2O_2) production; (G) aconitase activity measured in human neonatal dermal fibroblasts (Fn) and patient fibroblasts (P1) and (P2) lysates; (H) degree of protein carbonylation in human neonatal dermal fibroblasts (Fn) and patient fibroblasts (P1) and (P2); (I) activity of mitochondrial ATP synthase as determined by a blue native in-gel activity assay; Bars are averages of at least three independent measurements and are expressed as a percentage of control (Fn) cells for each parameter. Statistically significant differences between Fn and NARP (P1 and P2) cell lines are indicated $^*P < 0.05$.

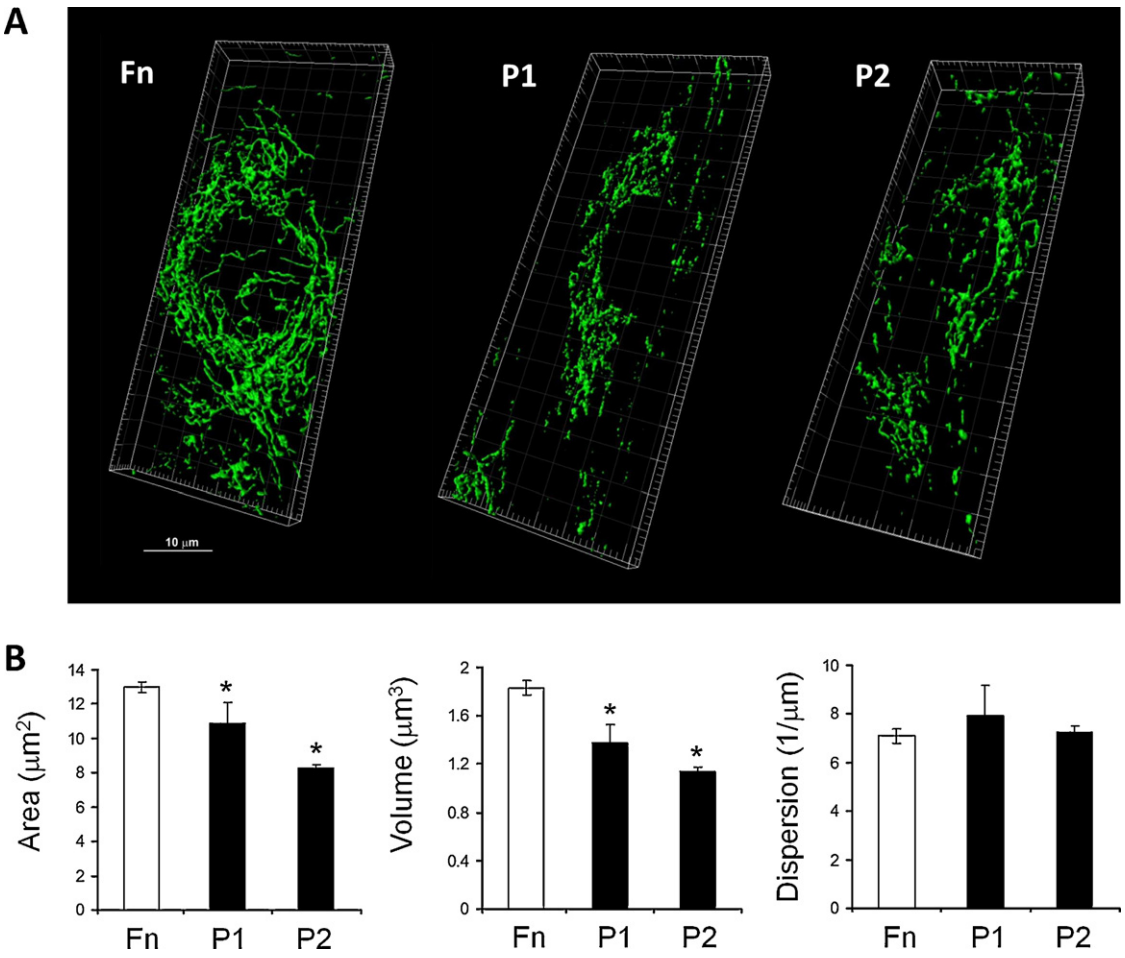

Fig. 2. Mitochondrial structure and structural mitochondrial parameters in control and patient fibroblasts. (A) 3D structure of mitochondria; (B) structural parameters (area, volume and dispersion) in control human neonatal dermal fibroblasts (Fn) and patient fibroblasts (P1) and (P2). The cells were seeded on glass coverslips, fixed, labelled and imaged as described in Section 4. A typical picture of mitochondrial structure is shown. Bars are averages of three independent. Statistically significant differences between Fn and NARP (P1 and P2) cell lines are indicated $^{*}P < 0.05$.

participate in the generation of oxygen free radicals not only by a direct interaction with cytochrome c (Giorgio et al., 2005) but also by establishing a connection with mitochondrial p53 and Mn-superoxide dismutase (Pani and Galeotti, 2011). However, recent findings cast some doubts on whether p66Shc enters the mitochondria, which would exclude a direct interaction with cytochrome c, or associates with the outer mitochondrial membrane (Wieckowski et al., 2009).

In our previous study, we demonstrated that intracellular oxidative stress related to respiratory chain dysfunction can trigger the phosphorylation of p66Shc at Ser36 (Lebiedzinska et al., 2010). This finding indicates that intracellular oxidative stress can also activate the p66Shc phosphorylation pathway. The results presented in the current manuscript refer to a situation in which intracellular oxidative stress is not related to the defective mitochondrial respiratory chain but is rather the consequence of mitochondrial hyperpolarisation. A detailed characterisation of our experimental model revealed a small (statistically not significant when measured with TMRM) but statistically significant measured with JC-1 probe increase in the mitochondrial membrane potential in NARP fibroblasts. This was accompanied by the decreased activity of the mitochondrial respiratory chain as a consequence of ATP synthase inhibition and mitochondrial coupling. The mitochondrial coupling was confirmed by a higher NADH/NAD ratio, in both NARP patients compared with the control fibroblasts. We also demonstrated an alteration of mitochondrial Ca^{2+} homeostasis in NARP fibroblasts that manifested as a decrease in Ca^{2+} uptake by the mitochondria. Moreover, in NARP fibroblasts, the mitochondrial network was fragmented, which can serve as evidence of enhanced oxidative stress (Sardão et al., 2007). Measurement of superoxide production in the mitochondrial matrix with the use of Mitosox red suggests a relation with increased mitochondrial superoxide production. Unfortunately, Mitosox derived fluorescence depends both on the levels of mt. $O_2^{\bullet -}$ and mitochondrial membrane potential due to the fact that its accumulation depends directly on the mitochondrial membrane potential. Therefore, Mitosox red only gives a qualitative assessment of mitochondrial superoxide generation. For this reason, to justify and demonstrate increased level of mt. $O_2^{\bullet -}$, we measured the activity of aconitase, an enzyme present in the mitochondrial matrix compartment and involved in the tricarboxylic acid cycle. Aconitase is extremely sensitive to ROS due to the presence of a labile iron-sulphur cluster (Gardner, 2002). Therefore, its activity may be used to reflect the level of ROS inside the mitochondria. Decreased aconitase activity supported the Mitosox data concerning the possible higher level of mt. $O_2^{\bullet -}$ observed in the mitochondrial matrix.

All this, together with oxidatively damaged proteins in NARP fibroblasts confirmed the relationship between the mitochondrial membrane potential and mitochondrial ROS production that was described by Korshunov et al. (1997). The increased mitochondrial superoxide production in NARP fibroblasts was accompanied by a high level of SOD2, which suggests an adaptation to the

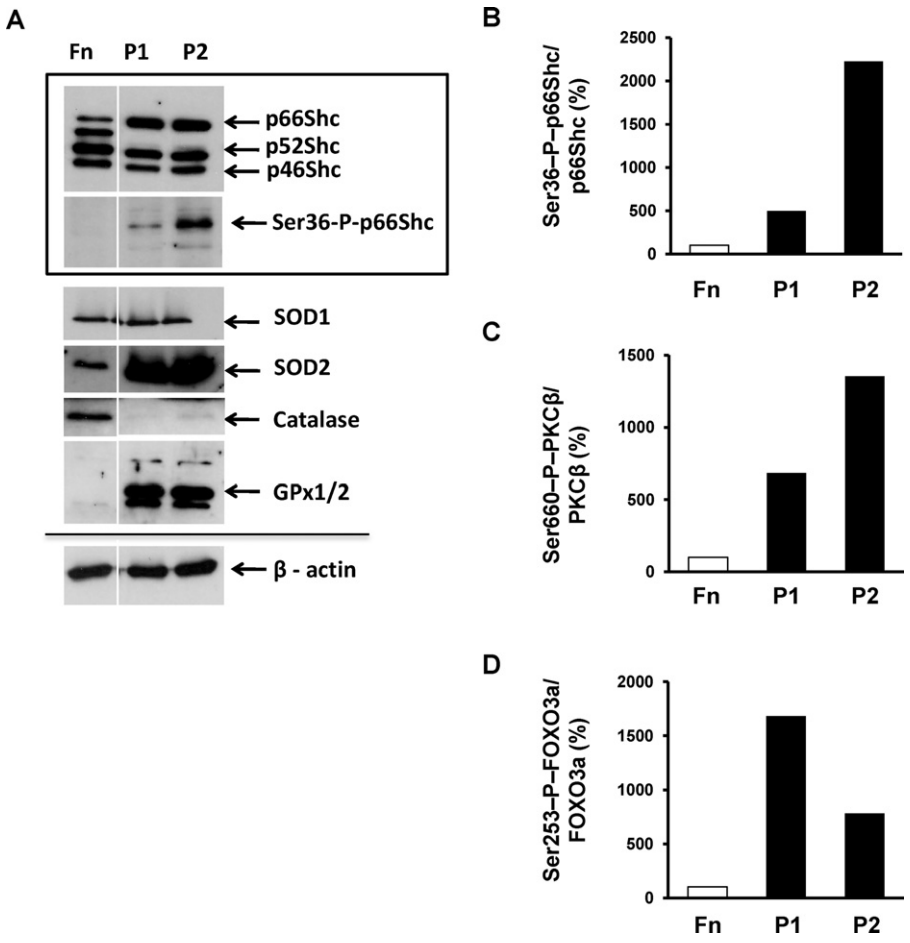

Fig. 3. Levels of Shc proteins and expression of antioxidant enzymes in control and patient fibroblasts. (A) The expression profiles of Shc proteins (p66Shc, p52Shc, p46Shc) and Ser36-P-p66Shc in human neonatal dermal fibroblasts (Fn) and patient fibroblasts (P1) and (P2) were estimated as described in Section 4; (B) the expression profiles of cytosolic superoxide dismutase (SOD1), mitochondrial superoxide dismutase (SOD2), catalase and glutathione peroxidase (GPx) were estimated as described in Section 4; (C) the level of Ser36 phosphorylation on p66Shc and the PKCβ phosphorylation index in human neonatal dermal fibroblasts (Fn) and patient fibroblasts (P1) and (P2) were estimated as described in Section 4. A typical result of immunoblots is shown. In (B, C and D) bars are averages of two independent experiments.

elevated level of superoxide in the mitochondrial matrix. Similarly, Geromel et al. (2001) have found increased activity of SOD2, which was accompanied by an increased amount of its mRNA in the NARP fibroblasts. Similarly to the data presented by Mattiazzi et al. (2004) we found no change in the predominantly cytosolic SOD1. Additionally, the transcription factor FOXO3a, which is controlled by p66Shc and is responsible for the regulation of SOD2 expression, was inactivated in NARP fibroblasts (see Supplementary Figure 5). We detected low levels of catalase, which is involved in the detoxification of H_2O_2, in NARP cells. However, the increased levels of GPx1 and 2 in these cells could potentially provide a functional substitute for catalase activity. Similar to catalase, GPx1 and 2 are responsible for H_2O_2 elimination, but FOXO3a does not control the expression of the GPx proteins. This finding may explain the lower level of H_2O_2 production in our NARP fibroblasts. However, we did not find any explanation for the observed lower level of cytosolic superoxide in the NARP cells, especially if the SOD1 level was found to be the same in control and NARP cells.

In our experimental model of endogenous oxidative stress resulting from mitochondrial hyperpolarisation, we observed increased activity of PKCβ and an increase in p66Shc phosphorylation at Ser36. Interestingly, we observed a similar effect upon the inhibition of ATP synthase in control cells by oligomycin. In oligomycin-treated cells, we observed increased membrane potential and mitochondrial superoxide production, which clearly shows a link between the mitochondrial hyperpolarisation and p66Shc phosphorylation at Ser36. It has been proposed by Mattiazzi et al. (2004) that the increase of ROS production in the control cells treated with oligomycin was smaller than spontaneously occurring in T8993G mutant cybrids used for the studies. They concluded that the inhibition of the ATP synthase is not the only cause of increased ROS production in NARP cells and can be also a reason of insufficient antioxidant defences activity (i.e. lower catalase level and not upregulated SOD1 level presented in our studies). Moreover, as it has been frequently described that in response to oxidative stress, high levels of p66Shc phosphorylation at Ser36 promote an additional increase in mitochondrial ROS generation (Arany et al., 2010; Lebiedzinska et al., 2010; Le et al., 2001; Yang and Horwitz, 2002) and influence the levels of antioxidant enzymes. If p66Shc phosphorylation at Ser36 is an important factor in the pathology of oxidative stress, its inhibition in NARP fibroblasts should at least partially alleviate the production of reactive oxygen species. In particular, the treatment of NARP fibroblasts with SkQ (a plastoquinone-derivative mitochondrial-targeted antioxidant) decreased p66Shc phosphorylation in NARP fibroblasts (Fig. 4). This demonstrates that mitochondrial oxidative stress can be a primary event in the activation of p66Shc, although at this point we cannot rule out other sources as well. Similarly, the inhibition of p66Shc phosphorylation by hispidin, which is an inhibitor of PKCβ, decreased mitochondrial superoxide production in both NARP cell lines. Surprisingly, as we previously observed in the fibroblasts of patients with combined mitochondrial defects,

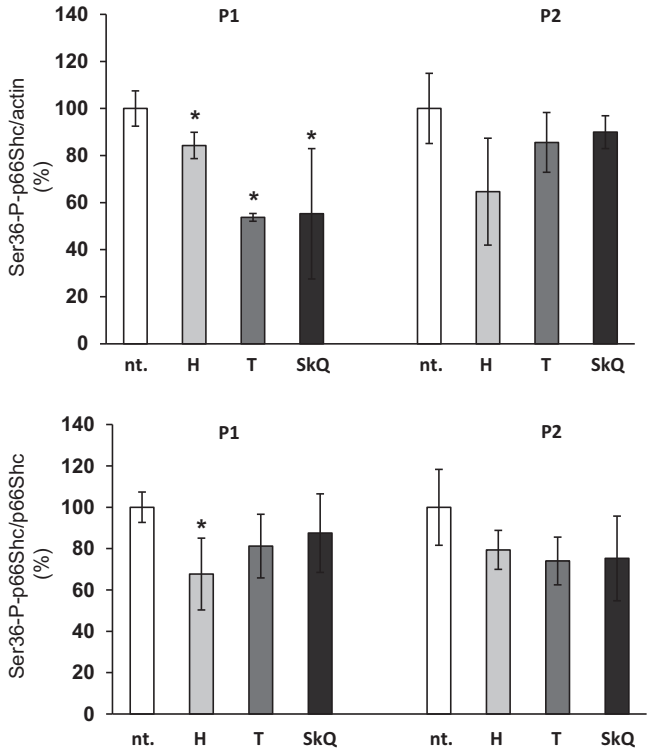

Fig. 4. Effect of hispidin, trolox and SkQ treatment on the Ser36-phosphorylation of p66Shc in NARP fibroblasts. The p66Shc phosphorylation at Ser36 in patient fibroblasts (P1) and (P2) treated with trolox (T), hispidin (H) and SkQ (SkQ) was estimated as described in Section 4. The untreated cells are denoted by (nt). Western blot scans were analysed using NIH ImageJ software; Bars are averages of three independent experiments and are expressed as a percentage of untreated (nt.) P1 and P2 cells for each treatment respectively. Statistically significant differences between untreated and treated NARP (P1 and P2) cell lines are indicated $^{*}P < 0.05$.

hispidin also increased the hydrogen peroxide production in NARP fibroblasts (Lebiedzinska et al., 2010), but the possible mechanisms of this phenomenon should be elucidated in detail in further studies. The differences in the response for the treatment between the two NARP cell lines can be explained by previously observed high variations among cell lines carrying the same T8993G mutation (D'Aurelio et al., 2010).

From the data presented in this work, we can conclude that an increase in ROS production related to mitochondrial membrane hyperpolarisation is also responsible for the p66Shc phosphorylation at Ser36. Inhibition of p66Shc phosphorylation by hispidin results in decreased mitochondrial superoxide anion production, which acts downstream of p66Shc activation. The pro-oxidant properties of p66Shc can induce a vicious cycle of ROS production that leads to the escalation of intracellular oxidative stress. The inhibition of p66Shc phosphorylation at Ser36 seems to be a viable strategy to decrease the severity of the oxidative stress that accompanies mitochondrial pathologies.

4. Materials and methods

4.1. Ethics

The present studies with human fibroblasts were performed in accordance with the Declaration of Helsinki of the World Medical Association and were approved by the Committee of Bioethics at the Children's Memorial Health Institute. Informed consent was obtained from the parents before any biopsy or molecular analysis was performed.

4.2. Fibroblast cultures

Human skin fibroblasts were grown from explants of skin biopsies in standard Dulbecco's modified Eagle medium (DMEM) with high glucose (4.5 g/l), 5 mM sodium pyruvate and 2 mM L-glutamine (Lonza) that was supplemented with 10% (v/v) foetal bovine serum (Gibco) and 1% penicillin/streptomycin solution (Sigma–Aldrich) and an atmosphere of 5% (v/v) carbon dioxide in air at 37 °C. Human neonatal dermal fibroblasts (NHDF, Cat. n. CC-2509, Lonza) were used as a healthy control (Fn). Additionally, NHDF adult dermal fibroblasts (Cat. n. CC-2511, Lonza) (C2) and human skin fibroblasts from a healthy volunteer (C3) were used for a comparison with the control (Fn) healthy fibroblasts. The medium was changed every two days. The cells were cultured on 10-cm plates until they reached confluence. The cells were passaged onto multiwell plates 2 days prior to the measurement of ROS and mitochondrial parameters, and the medium was changed the day before the experiment.

Optionally, Dulbecco's modified Eagle medium was supplemented with 3 μM hispidin (Sigma–Aldrich), 250 μM Trolox (Sigma–Aldrich), or 1 nM SkQ (V. Skulachev, Moscow), and the cells were cultured for 5 days. The growth medium that was supplemented with the effectors was changed every two days.

4.3. Cytochemistry

Two days before an experiment, the cells were plated in Lab-Tek II chambers (Nalge Nunc International, USA) in the culture medium and grown under standard conditions for 48 h. The following protocols were performed.

4.3.1. Haematoxylin and eosin (H&E) staining

The cells were washed with PBS, fixed in chilled methanol for 10 min, washed with PBS and stained with haematoxylin (Sigma #MHS-32). The cells were then washed for 5 min with tap water and stained with a water solution of eosin (Sigma #HT110-2-32). The cells were mounted on glass slides with DPX.

4.3.2. Succinate dehydrogenase activity (SDH)

The histochemical staining for SDH activity was performed according to a modification of the method originally described by Seligman et al. (1968) and Dubowitz (1985). The cells were washed with PBS and incubated in 50 mM Tris–HCl, pH 7.54, that was supplemented with 50 mM succinate and 0.25 mg/ml nitrotetrazolium blue for 1 h at 37 °C in a humid chamber. The slides were then washed three times with deionised water and mounted on glass slides with Dako Faramount aqueous mounting medium.

4.3.3. Oil Red O staining

The cells were washed with PBS, fixed in 10% buffered formalin, and preincubated in an 85% water solution of propylene glycol (1,2-propanediol). The slides were stained with a 0.5% solution of Oil Red O (Sigma–Aldrich) in 100% propylene glycol. The slides were then washed with deionised water, and the nuclei were stained with haematoxylin. Finally, the slides were mounted on glass slides with Dako Faramount aqueous mounting medium.

4.3.4. NADH dehydrogenase staining

The cells were washed three times with PBS and incubated in 50 mM Tris–HCl, pH 7.54, that was supplemented with 0.5 mg/ml NADH and 1 mg/ml nitrotetrazolium blue for 1 h at 37 °C in a humid chamber. The slides were then washed three times with deionised

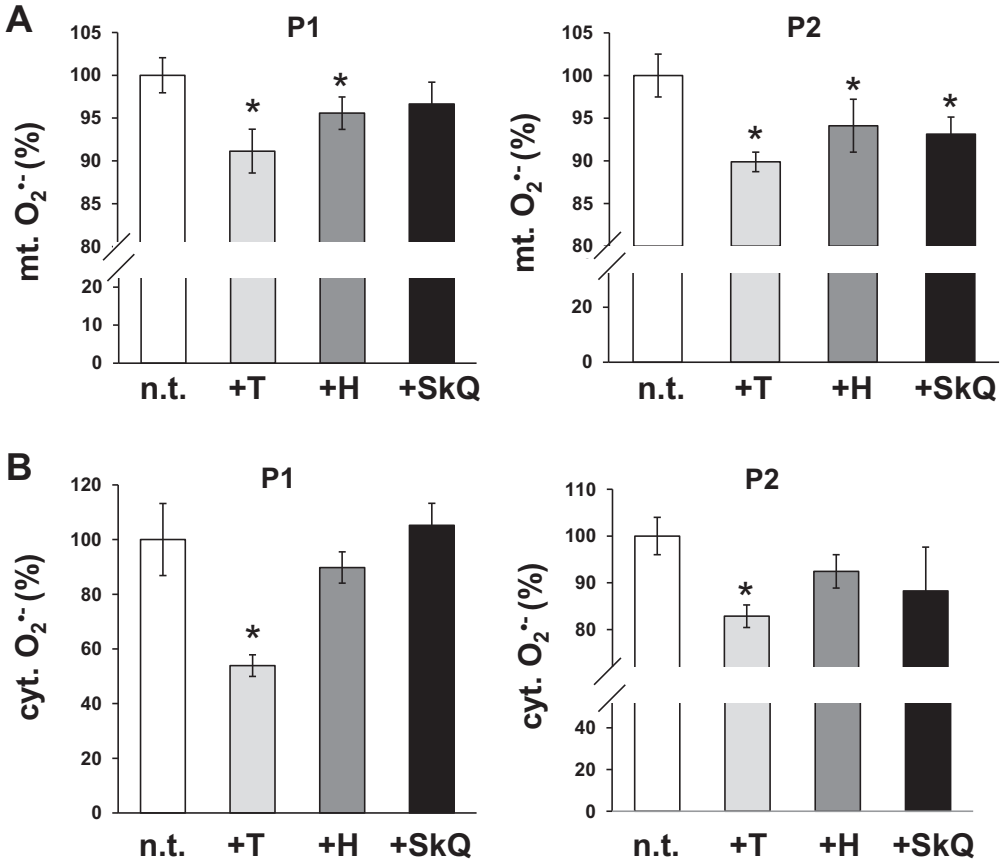

Fig. 5. Effect of trolox, hispidin and SkQ treatment on cytosolic and mitochondrial superoxide production in patient fibroblasts. (A) The effect of trolox (T), hispidin (H) and SkQ (SkQ) on mitochondrial superoxide production; (B) the effect of trolox (T), hispidin (H) and SkQ (SkQ) on cytosolic superoxide production; cells not treated (nt). The patient fibroblasts (P1) and (P2) were treated with trolox, hispidin and SkQ as described in Section 4. Bars are averages of at least three independent experiments and are expressed as a percentage of untreated (nt.) P1 and P2 cells for each treatment respectively. Statistically significant differences between untreated and treated NARP (P1 and P2) cell lines are indicated $^*P < 0.05$.

water and mounted on glass slides with Dako Faramount aqueous mounting medium.

4.4. Measurement of respiratory chain activity

Fibroblasts that had been grown in 24-well plates were washed twice with PBS and then incubated in PBS containing 5 mM glucose and 6 μM resazurin (Sigma–Aldrich). The fluorescence was recorded immediately thereafter in a microplate reader (Infinite M200, Tecan, Austria) with excitation and emission wavelengths of 510 nm and 595 nm, respectively. To determine the level of nonspecific reaction, the cells were pre-incubated with medium containing 2 mM KCN for 15 min.

4.5. Measurement of mitochondrial membrane potential ($mt\Delta\Psi$)

Fibroblasts grown in 24-well plates were washed twice with PBS to remove the medium and then incubated in the presence of 20 nM TMRM Sigma in PBS containing 5 mM glucose for 20 min at 37 °C. The cells were washed twice with PBS. The fluorescence was then measured in a microplate reader (Infinite M200, Tecan, Austria) with wavelengths of 544 nm (excitation)/590 nm (emission). Moreover, mitochondrial membrane potential has been evaluated with the use of 5,5′,6,6′-tetrachloro-1,1′,3,3′-tetraethylbenzimidazolylcarbocyanine iodide (JC-1) fluorescent probe. Fibroblasts grown in 24-well plates were washed twice with PBS to remove the medium and then incubated in the presence of 10 μM JC-1 in PBS containing 5 mM glucose for 10 min at 37 °C. The cells were washed twice with PBS and the green and red fluorescence was recorded in a microplate reader (Infinite M200, Tecan, Austria), respectively, at 485 nm excitation/520 nm emission and at 535 nm excitation/635 nm emission wavelengths.

4.6. Measurement of NAD(P)H and FAD autofluorescence

The autofluorescence was imaged using a Zeiss 510 META confocal system on a heated stage at 37 °C. NAD(P)H was excited by a 351 nm UV laser (Coherent), and the emitted light was collected with a 435–485 nm band pass filter. The FAD autofluorescence was detected by line excitation with a 488 nm argon laser, and the emitted light was collected with a 510 nm long pass filter. To measure the relative redox state (denoted as the redox index) of the NAD(P)/NAD(P)H pair, the signal was corrected for bleaching and normalised to the maximally oxidised (in the presence of 1 μM FCCP) and maximally reduced (in the presence of 1 μM rotenone) signals, which were measured after each run.

4.7. Measurement of H_2O_2 production

The rate of H_2O_2 production was measured with the ROS-sensitive fluorescent probe 5CM-H_2DCFDA (Invitrogen). The cells were grown in 24-well plates and treated with 2 μM CM-H_2DCFDA. The kinetics of the fluorescence increase was then recorded in a microplate reader for 30 min with excitation and emission wavelengths of 495 nm and 520 nm, respectively.

4.8. Measurement of mitochondrial superoxide ($mtO_2^{\bullet-}$) production

Fibroblasts grown in 24-well plates were incubated for 10 min at 37 °C in the presence of 5 μM Mitosox red (Invitrogen) in PBS containing 5 mM glucose. The cells were washed twice with PBS, and the fluorescence was recorded in a microplate reader with excitation and emission wavelengths of 510 nm excitation and 595 nm, respectively.

4.9. Measurement of cytosolic superoxide ($cytO_2^{\bullet-}$) production

Fibroblasts grown in 24-well plates were incubated for 20 min at 37 °C in the presence of 0.5 μM dihydroethidium (DHE, Invitrogen) in PBS containing 5 mM glucose. The cells were washed twice with PBS, and the fluorescence was recorded in a microplate reader with excitation and emission wavelengths of 535 nm and 635 nm, respectively.

4.10. Measurement of the aconitase activity

The aconitase activity was measured spectrophotometrically in whole cell lysates with the use of the Aconitase Enzyme Activity Microplate Assay Kit (Mitosciences) following the standard protocol of the manufacturer.

4.11. Measurement of mitochondrial calcium uptake

Cells grown on 13 mm round glass coverslips at 50% confluence were infected with the adenovirus expressing the mitochondrial aequorin chimera. All measurements were carried out in KRB (125 mM NaCl, 5 mM KCl, 1 mM $MgSO_4$, 1 mM Na_2HPO_4, 5.5 mM glucose, 20 mM $NaHCO_3$, 2 mM L-glutamine and 20 mM HEPES pH 7.4, and was supplemented with 1 mM $CaCl_2$). Agonist was added to the same medium. The experiments were terminated by lysing the cells with 100 μM digitonin in a hypotonic Ca^{2+}-rich solution (10 mM $CaCl_2$ in H_2O), thus discharging the remaining aequorin pool. The light signal was collected and calibrated into $[Ca^{2+}]$ values, as previously described (Pinton et al., 2007).

4.12. Detection of oxidatively modified proteins

The levels of oxidised proteins were estimated using the OxyBlot protein oxidation detection kit (Chemicon). Aliquots of 25 μg of protein were separated on a 10% SDS polyacrylamide gel, and the standard protocol of the manufacturer was followed.

4.13. Sample preparation for Western blots

The cell pellets were resuspended in cold lysis buffer (50 mM Tris, pH 7.5, 150 mM NaCl, 1% Triton, 0.1% SDS, 1% sodium deoxycholate) with protease inhibitor cocktail (Sigma–Aldrich) and phosphatase inhibitor cocktail (Sigma–Aldrich). The samples were incubated on ice for 15 min and then centrifuged at 14,000 × *g* for 20 min at 4 °C to remove insoluble cellular debris. The protein concentration in the supernatant was determined using the Bradford method. The samples for SDS-PAGE were denatured in reducing Laemmli loading buffer in 95 °C or 45 °C (for OXPHOS complex detection) for 5 min.

4.14. Western blotting

The cell lysates (25–50 μg protein) were separated by SDS-PAGE in 8% or 10% polyacrylamide gels (BioRad) and transferred onto PVDF membranes (BioRad). The membranes were blocked using 2% non-fat milk (BioRad) in TBS buffer containing 0.01% Tween 20 (TBS-T, Sigma–Aldrich) for 1 h. The following antibodies were used for protein detection: p66Shc (BD Biosciences) and Ser36-P-p66Shc (Calbiochem) monoclonal antibodies (both diluted 1:1000), SOD1 rabbit polyclonal antibody (1:5000; Santa Cruz), SOD2 goat polyclonal antibody (1:500; Abcam), catalase monoclonal antibody (1:1000; Santa Cruz), GPx1/2 (1:500; Santa Cruz), FOXO3a (1:1000; Abcam), Ser253-P-FOXO3a (1:1000; Abcam), PKCβ (1:500; Santa Cruz), Ser660-P-PKCβ (1:1000; Cell Signaling) and monoclonal β-actin peroxidase conjugated antibody (1:10,000, Sigma–Aldrich), followed by the appropriate secondary HRP-conjugated antibody (1:5000) (Santa Cruz), all in 2% milk in TBS-T buffer.

4.15. Analysis of mitochondrial network morphology

To label mitochondria, the cells were incubated according to the manufacturer's instructions with the MitoTracker Red CMXRos (Invitrogen) probe, which passively diffuses across the plasma membrane and accumulates in polarized mitochondria. After the staining, the coverslips were placed in an acquisition chamber mounted under the microscope. Short imaging sessions to evaluate the morphology and motility of mitochondria were performed at 37 °C and under a stable 5% CO_2 concentration. The images were acquired using a Leica TCS SP5 confocal microscope (Leica) with a PL Apo: 63x/1.32 NA oil immersion objective using the 561 nm line of a diode pumped solid state laser with 10% transmission and a pixel count of 1024 × 1024. A series of z-stacks was acquired for a cell with a step of 0.2 μm and additional digital zoom to provide a final lateral resolution of 0.08 μm per pixel. The confocal images with the highest resolution were restored by three-dimensional (3D) deconvolution using Huygens Professional software (Scientific Volume Imaging, Hilversum, Netherlands, http://www.svi.nl/) that applied a classic maximum-likelihood estimation algorithm and an automatically generated point-spread function. The 3D reconstructions of the confocal images and the quantitative morphometric analysis of the mitochondria were performed offline with Imaris software provided by Biplane.

4.16. Blue native electrophoresis and in-gel activity assay

The blue native electrophoresis was performed as previously described previously (Karkucinska-Wieckowska et al., 2006). To visualise the activities of the monomeric, dimeric and multimeric forms of mitochondrial ATPase, the gel was incubated at 35 °C with a solution containing 35 mM Tris–HCl, 270 mM glycine, 14 mM $MgSO_4$, 0.2% $Pb(NO_3)_2$ and 8 mM ATP (pH 7.8). The incubation was terminated when the white bands that represent the active mitochondrial ATPase became visible (approximately 12 h).

4.17. Estimation of mtDNA copy number

The mtDNA was isolated by phenol-chloroform extraction, which was followed by SYBR Green qPCR amplification with primers that annealed onto the UCP2 nuclear gene (intron 2 and exon 3) and the ND5 mitochondrial gene (bp 11,092–11,191, according to the Genebank sequence from the National Centre for Biotechnology Information, USA). The ratio between the ND5 amplicon and half of the nuclear amplicon amount was defined as the mtDNA copy number per cell.

4.18. Statistical analysis

The differences in the band densities were analysed using NIH ImageJ software. The data obtained from the microplate reader (Infinite M200, Tecan, Austria) were analysed using Microsoft Excel 2005, Statistically significant differences between control (Fn) and

NARP patient cell lines were estimated by unpaired two tailed Student's *t*-test. A level of confidence of $P < 0.05$ was adopted. Where appropriate, we applied 1-way ANOVA with post hoc analysis. Significance levels were set at $P < 0.05$.

Conflict of interest

The authors have declared no conflicts of interest.

Acknowledgements

This work was supported by the Polish Ministry of Science and Higher Education under grant NN407 075 137 for ML, AKW, JMS, JD, MP and MRW. JMS was also supported by a PhD fellowship from the Foundation for Polish Science, EU, European Regional Development Fund and Operational Programme 'Innovative economy'. ML was the recipient of a fellowship from the Foundation for Polish Science (Program Start) and the L'Oreal Fellowship for Women in Science. PP was supported by the Italian Association for Cancer Research (AIRC), Telethon (GGP09128), local funds from the University of Ferrara, the Italian Ministry of Education, University and Research (COFIN), the Italian Cystic Fibrosis Research Foundation and the Italian Ministry of Health. GS was supported by Parkinson's UK (grant G-0905). JT and PJ were supported by grant P305/12/1247 from the Grant Agency of the Czech Republic, GACR. This work was also supported by the PhD fellowship SFRH/BD/48133/2008 for CD.

Appendix A. Supplementary data

Supplementary data associated with this article can be found, in the online version, at http://dx.doi.org/10.1016/j.biocel.2012.07.020.

References

Arany I, Faisal A, Clark JS, Vera T, Baliga R, Nagamine Y. p66SHC-mediated mitochondrial dysfunction in renal proximal tubule cells during oxidative injury. American Journal of Physiology: Renal Physiology 2010;298(5):1214–21.

Craig K, Elliott HR, Keers SM, Lambert C, Pyle A, Graves TD, et al. Episodic ataxia and hemiplegia caused by the 8993T->C mitochondrial DNA mutation. Journal of Medical Genetics 2007;44(12):797–9.

D'Aurelio M, Vives-Bauza C, Davidson MM, Manfredi G. Mitochondrial DNA background modifies the bioenergetics of NARP/MILS ATP6 mutant cells. Human Molecular Genetics 2010;19(2):374–86.

Dubowitz V. Muscle biopsy: a practical approach. London; Philadelphia: Bailliere Tindall; 1985.

Gardner PR. Aconitase: sensitive target and measure of superoxide. Methods in Enzymology 2002;349:9–23.

Giorgio M, Migliaccio E, Orsini F, Paolucci D, Moroni M, Contursi C, et al. Electron transfer between cytochrome c and p66Shc generates reactive oxygen species that trigger mitochondrial apoptosis. Cell 2005;122(2):221–33.

Geromel V, Kadhom N, Cebalos-Picot I, Ouari O, Polidori A, Munnich A, et al. Superoxide-induced massive apoptosis in cultured skin fibroblasts harboring the neurogenic ataxia retinitis pigmentosa (NARP) mutation in the ATPase-6 gene of the mitochondrial DNA. Human Molecular Genetics 2001;10(11):1221–8.

Hu Y, Wang X, Zeng L, De-Yu Cai D-Y, Sabapathy K, Goff SP, et al. ERK phosphorylates p66shcA on Ser36 and subsequently regulates p27kip1 expression via the Akt-FOXO3a pathway: implication of p27kip1 in cell response to oxidative stress. Molecular Biology of the Cell 2005;16(8):3705–18.

Jones DP. Disruption of mitochondrial redox circuitry in oxidative stress. Chemico-Biological Interactions 2006;163(1-2):38–53.

Karkucinska-Wieckowska A, Czajka K, Wasilewski M, Sykut-Cegielska J, Pronicki M, Pronicka E, et al. Blue Native Electrophoresis: an additional useful tool to study deficiencies of mitochondrial respiratory chain complexes. Annals of Diagnostic Pediatric Pathology 2006;10(3–4):89–92.

Kakkar P, Singh BK. Mitochondria: a hub of redox activities and cellular distress control. Molecular and Cellular Biochemistry 2007;305(1-2):235–53.

Khanday FA, Santhanam L, Kasuno K, Yamamori T, Naqvi A, DeRicco J, et al. Sos-mediated activation of rac1 by p66shc. Journal of Cell Biology 2006;172(6):817–22.

Koch OR, Fusco S, Ranieri SC, Maulucci G, Palozza P, Larocca LM, et al. Role of the life span determinant P66(shcA) in ethanol-induced liver damage. Laboratory Investigation 2008;88(7):750–60.

Korshunov SS, Skulachev VP, Starkov AA. High protonic potential actuates a mechanism of production of reactive oxygen species in mitochondria. FEBS Letters 1997;416(1):15–8.

Kowaltowski AJ, de Souza-Pinto NC, Castilho RF, Vercesi AE. Mitochondria and reactive oxygen species. Free Radical Biology and Medicine 2009;47(4):333–43.

Lam EW, Francis RE, Petkovic M. FOXO transcription factors: key regulators of cell fate. Biochemical Society Transactions 2006;34(Pt 5):722–6.

Le S, Connors TJ, Maroney AC. c-Jun N-terminal kinase specifically phosphorylates p66ShcA at serine 36 in response to ultraviolet irradiation. Journal of Biological Chemistry 2001;276(51):48332–6.

Lebiedzinska M, Duszynski J, Rizzuto R, Pinton P, Wieckowski MR. Age-related changes in levels of p66Shc and serine 36-phosphorylated p66Shc in organs and mouse tissues. Archives of Biochemistry and Biophysics 2009;486(1):73–80.

Lebiedzinska M, Karkucinska-Wieckowska A, Giorgi C, Karczmarewicz E, Pronicka E, Pinton P, et al. Oxidative stress-dependent p66Shc phosphorylation in skin fibroblasts of children with mitochondrial disorders. Biochimica et Biophysica Acta 2010;1797(6-7):952–60.

Lenaz G, Baracca A, Carelli V, D'Aurelio M, Sgarbi G, Solaini G. Bioenergetics of mitochondrial diseases associated with mtDNA mutations. Biochimica et Biophysica Acta 2004;1658(1–2):89–94.

Lotti LV, Lanfrancone L, Migliaccio E, Zompetta C, Pelicci G, Salcini AE, et al. Sch proteins are localized on endoplasmic reticulum membranes and are redistributed after tyrosine kinase receptor activation. Molecular and Cellular Biology 1996;16(5):1946–54.

Luzi L, Confalonieri S, Di Fiore PP, Pelicci PG. Evolution of Shc functions from nematode to human. Current Opinion in Genetics and Development 2000;10(6):668–74.

Mancuso M, Orsucci D, Coppedè F, Nesti C, Choub A, Siciliano G. Diagnostic approach to mitochondrial disorders: the need for a reliable biomarker. Current Molecular Medicine 2009;9(9):1095–107.

Mattiazzi M, Vijayvergiya C, Gajewski CD, DeVivo DC, Lenaz G, Wiedmann M, et al. The mtDNA T8993G (NARP) mutation results in an impairment of oxidative phosphorylation that can be improved by antioxidants. Human Molecular Genetics 2004;13(8):869–79.

Migliaccio E, Giorgio M, Mele S, Pelicci G, Reboldi P, Pandolfi PP, et al. The p66shc adaptor protein controls oxidative stress response and life span in mammals. Nature 1999;402(6759):309–13.

Migliaccio E, Mele S, Salcini AE, Pelicci G, Lai KM, Superti-Furga G, et al. Opposite effects of the p52shc/p46shc and p66shc splicing isoforms on the EGF receptor-MAP kinase-fos signalling pathway. EMBO Journal 1997;16(4):706–16.

Nemoto S, Finkel T. Redox regulation of forkhead proteins through a p66shc-dependent signaling pathway. Science 2002;295(5564):2450–2.

Pagnin E, Fadini G, de Toni R, Tiengo A, Calo L, Avogaro. A Diabetes induces p66shc gene expression in human peripheral blood mononuclear cells: relationship to oxidative stress. Journal of Clinical Endocrinology and Metabolism 2005;90:1130–6.

Pani G, Galeotti T. Role of MnSOD and p66shc in mitochondrial response to p53. Antioxidants and Redox Signalling 2011;15(6):1715–27.

Pani G, Koch OR, Galeotti T. The p53-p66shc-Manganese Superoxide Dismutase (MnSOD) network: a mitochondrial intrigue to generate reactive oxygen species. International Journal of Biochemistry and Cell Biology 2009;41(5):1002–5.

Pelicci G, Lanfrancone L, Grignani F, McGlade J, Cavallo F, Forni G, et al. A novel transforming protein (SHC) with an SH2 domain is implicated in mitogenic signal transduction. Cell 1992;70(1):93–104.

Pellegrini M, Pacini S, Baldari CT. p66SHC: the apoptotic side of Shc proteins. Apoptosis 2005;10(1):13–8.

Pereira CV, Moreira AC, Pereira SP, Machado NG, Carvalho FS, Sardão VA, et al. Investigating drug-induced mitochondrial toxicity: a biosensor to increase drug safety? Current Drug Safety 2009;4(1):34–54.

Pinton P, Rimessi A, Marchi S, Orsini F, Migliaccio E, Giorgio M, et al. Protein kinase C beta and prolyl isomerase 1 regulate mitochondrial effects of the life-span determinant p66Shc. Science 2007;315(5812):659–63.

Purdom S, Chen QM. Linking oxidative stress and genetics of aging with p66Shc signaling and forkhead transcription factors. Biogerontology 2003;4(4):181–91.

Sardão VA, Oliveira PJ, Holy J, Oliveira CR, Wallace KB. Vital imaging of H9c2 myoblasts exposed to tert-butylhydroperoxide-characterization of morphological features of cell death. BMC Cell Biology 2007;8:11.

Seligman AM, Karnovsky MJ, Wasserkrug HL, Hanker JS. Nondroplet ultrastructural demonstration of cytochrome oxidase activity with a polymerizing osmiophilic reagent, diaminobenzidine (DAB). Journal of Cell Biology 1968;38(1):1–14.

Smith WW, Norton DD, Gorospe M, Jiang H, Nemoto S, Holbrook NJ, et al. Phosphorylation of p66Shc and forkhead proteins mediates Abeta toxicity. Journal of Cell Biology 2005;169(2):331–9.

Suski JM, Lebiedzinska M, Bonora M, Pinton P, Duszynski J, Wieckowski MR. Relation between mitochondrial membrane potential and ROS formation. Methods in Molecular Biology 2012;810:183–205.

Wieckowski MR, Giorgi C, Lebiedzinska M, Duszynski J, Pinton P. Isolation of mitochondria-associated membranes and mitochondria from animal tissues and cells. Nature Protocols 2009;4(11):1582–90.

Yang CP, Horwitz SB. Distinct mechanisms of taxol-induced serine phosphorylation of the 66-kDa Shc isoform in A549 and RAW 264.7 cells. Biochimica et Biophysica Acta 2002;1590(1–3):76–83.

Zeviani M, Di Donato S. Mitochondrial disorders. Brain 2004;127(Pt 10):153–72.